

NON-LINEAR CONTROLS FOR ROBUSTNESS INVESTIGATION OF PMSG-BASED WIND TURBINE

Fadila TAHIRI¹, Abdelkader HARROUZ², Virgil DUMBRAVA³, Abdessalam BADOUD⁴, Moamen ALNATOOR¹

This paper presents robust controller techniques to improve the performance of WECSs. Firstly, vector control, which has shown fairly, limited results in terms of setpoint tracking. To overcome the insufficiencies of vector control, a backstepping type controller is proposed. The backstepping control allows operating the system in the best performance. This control less responds to the problems of regulation, tracking, and robustness with a parametric variation. Here we offer an adaptive control based on the fuzzy-backstepping control. The simulation results give an excellent result when applying the fuzzy-backstepping control, where shows perfect tracking responses and robust characteristics against statorique parameter variations.

Keywords: Wind, PMSG, vector control, backstepping, fuzzy-backstepping.

1. Introduction

With the growth of environmental problems resulting from the use of fossil fuels and increased energy consumption for the next decades, The majority of countries have entered into the dynamic to find solutions and in this framework, the use of renewable energies is an optimal solution for energy production [1]. The wind turbine, among renewable energy resources, has a large potential not to replace current energies but to compensate for the amortization of the ever-increasing demand. [2] Where its use has increased dramatically in recent years. Today, the globe has 743 GW of wind generating capacity, which helps to avoid around 1.1 billion tons of CO₂ [3.]. Wind turbines are power stations that are erected on the ground atmosphere and use wind energy from a multitude of levels. The motion of the wind is turned into mechanical energy by the rotor blades, which are subsequently transferred into electrical energy by the Permanent

¹ Eng., Dept. of Technology and Science, LDDI Laboratory, AHMED DRAIA University, Adrar, Algeria, e-mail: fad.tahiri@univ-adrar.edu.dz

² Prof., Dept. of Hydrocarbon and renewable Energy, LDDI Laboratory, AHMED DRAIA University, Adrar, Algeria, e-mail: abd.harrouz@univ-adrar.edu.dz

³ Prof., Dept. of Electric Power Systems, University POLITEHNICA of Bucharest, Romania, e-mail: v_dumbrava@yahoo.com

⁴ Prof., Dept. of Electrical Engineering, University of FERHAT ABBAS, Setif, Algeria, e-mail: badoudabde@yahoo.fr

Magnet Synchronous Generator (PMSG). Wind, according to Melo [4], is the movement of air in the atmosphere that occurs due to the uneven distribution of solar radiation and the heterogeneity of the underlying surface, thus uneven air temperature and atmospheric pressure changes. [4]

Currently, in the domain of renewable energy systems, variable speed generators are the most extensively employed [5], as a result of the evolution of electronics and permanent magnetic materials. In addition to having high thrust intensity, low energy loss, rapid dynamic response, and easy maintenance [6]. However, PMSG control remains complex due to the generator analytical model's non-linearity, parameter disturbances of external environmental elements, improper magnetic flux measurement, and previous control approaches have not entirely solved the performance of these problems [7]. Therefore, several research projects have been undertaken to optimize the performance of wind energy conversion systems WECSs [8, 9]. Among this research, the vector control or Field-Oriented Control (FOC). [10] The vector control proposed by Hasse in 1969 and Blaschke in 1972 allows AC drives to have a dynamic approach similar to that of DC drives [11]. This technique allows achieving a decoupling between the flux and the torque control [12],[13]. In this paper we applied this control technique, it was done by other researchers [14], [15] but after the results have been obtained, we note that there the disadvantages lie in the sensitivity to machine parametric variations. To improve the FOC the researchers suggest another technique; Mohammad Sadegh Eslahi et al [16], made a comparison between these three controls; FOC, Direct Power Control (DPC), and combination control, for PMSG. Salah Eddine Rhaili et al published a paper about the control of the WECSs using the Sliding Mode Control (SMC) [17]. Mohamed Nadour et al [18], proposed two techniques for controlling the Double Fed Induction Generator DFIG (PI controller, backstepping control). Youness El Mourabit et al [19] did a study focused on the PMSG of a wind turbine system using the backstepping control. We proposed a backstepping controller in this research that can transform the control law synthesis issue for the entire system into a control sequence synthesis problem for smaller systems by building it in stages using Lyapunov functions. Backstepping, by utilizing the latter's flexibility, can solve problems of regulation, tracking, and robustness in a less restricted manner than other techniques [13]. Today, new control strategies have been presented that are more adapted to overcoming the system's nonlinearities. Fuzzy logic control (FLC), in particular, offers an intriguing option. In comparison to PI controllers, this control provides superior transient response tracking and is less sensitive to parametric variation and disturbances. The FLC controller substitutes the PI controller in this approach; however, it requires a decoupling block identical to a PI [20]. The objective of our research is to create an adaptive control based on the fuzzy-backstepping control of PMSG. Even with parameter uncertainties, the

developed controller can track the reference signal rather effectively. The suggested technique is quite easy compared to existing based controller design schemes.

2. Modeling of wind Turbine

The kinetic energy of an air column of length dx (m), section S (m^2), air density ρ (kg/m^3), and wind speed v (m/s) is:

$$dE_c = \frac{1}{2} \cdot \rho \cdot S \cdot dx \cdot v^2 \quad (1)$$

The power coefficient C_p determines the proportion of power collected by a genuine wind rotor:

$$P_m = \frac{1}{2} \cdot C_p(\lambda) \cdot \rho \cdot S \cdot v^3 \quad (2)$$

The speed ratio λ is given by:

$$\lambda = \frac{\Omega \cdot R}{v} \quad (3)$$

Where, Ω represent the rotational speed (rad/s) and R represent the blade radius (m). The power coefficient has been calculated using particular readings obtained from a wind turbine by the following analytical equation:

$$C_p(\lambda, \beta) = (0.5 - 0.0167(\beta - 2)) \cdot \sin \left[\frac{\pi(\lambda + 0.1)}{18 - 0.3(\beta - 2)} \right] - 0.00184(\lambda - 3)(\beta - 2) \quad (4)$$

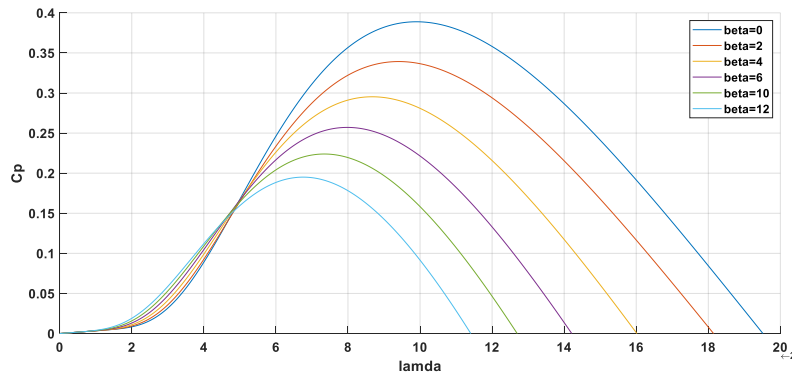


Fig. 1. Coefficient power as a function of ration speed

The mechanical torque T_m given as:

$$T_m = \frac{P_m}{\Omega} = \frac{R \cdot P_m}{\lambda \cdot v} = \frac{C_p}{\lambda} \cdot \frac{1}{2} \cdot \rho \cdot \pi \cdot R^3 \cdot v^2 \quad (5)$$

3. Modeling of PMSG

Model of the PMSG in a frame of (d, q) axis, associated to the rotor flux vector [8], taking into account the hypothesis commonly considered in the modeling of alternating current machines, are:

$$\begin{aligned}
 V_d &= -R_s \cdot I_d - L_d \frac{dI_d}{dt} + L_q \cdot \omega \cdot I_q \\
 V_q &= -R_s \cdot I_q - L_q \frac{dI_q}{dt} - L_d \cdot \omega \cdot I_d + \varphi_f \cdot \omega \\
 J \frac{d\Omega}{dt} &= T_m - T_{em} - F \cdot \Omega \\
 T_{em} &= \frac{3}{2} \cdot p \cdot [(L_q - L_d) \cdot I_d \cdot I_q + \varphi_f \cdot I_q] \\
 P &= T_{em} \cdot \Omega
 \end{aligned} \tag{6}$$

Where P, ω , p, J, φ_f , F, T_m , R_s , L_d and L_q represent the electromagnetic power, rotor angular velocity, number of pole pairs, rotor moment of inertia, permanent magnet flux, friction coefficient, mechanical torque, stator resistance and stator inductance of (d, q) axis respectively.

4. Vector control (FOC) of PMSG

The control of the oriented flux is a technique that introduces a method of decomposing the stator current vector into two components; one controls the flux and the other acts on the torque. The idea is to solve the problem of coupling between the two axes (d, q), where the torque is controlled by component (I_q), while the flux is controlled by (I_d). By controlling the quantities (I_d and I_q) acting directly on the voltages V_d and V_q .[22]

In this control technique $I_d = 0$, since it is constant, therefore the electromagnetic torque is directly proportional to I_q .

$$T_{em} = \frac{3}{2} \cdot p \cdot \varphi_f \cdot I_q \tag{7}$$

The machine model in the Park's reference is;

$$\begin{aligned}
 V_d &= -\omega \cdot L_d \cdot I_d + U_d \\
 V_q &= -\omega \cdot (\varphi_f + L_q \cdot I_q) + U_q
 \end{aligned} \tag{8}$$

On the other hand:

$$\begin{aligned} V_d &= R_s \cdot I_d + L_d \frac{dI_d}{dt} \Rightarrow V_d = (sL_d + R_s) \cdot I_d \\ V_q &= R_s \cdot I_q + L_q \frac{dI_q}{dt} \Rightarrow V_q = (sL_q + R_s) \cdot I_q \end{aligned} \quad (9)$$

Where; s; the variable of the Laplace transform.

Current regulators

From (9), the expressions for the currents is;

$$\begin{aligned} \frac{I_d}{V_d} &= \frac{1}{(sL_d + R_s)} \\ \frac{I_d}{V_d} &= \frac{1}{(sL_q + R_s)} \end{aligned} \quad (10)$$

As a result, we have two comparable PI regulators that are employed in two independent loops to control the component of the axes (d, q), as shown in fig.2. [23]

Speed control

The dynamics of the speed is demonstrated in:

$$J \frac{d\Omega}{dt} + F \cdot \Omega = T_m - T_{em} \quad (11)$$

Where;

$$\Omega = \frac{T_m - T_{em}}{J \cdot s + F} \quad (12)$$

To maintain the corresponding speed, the variable speed regulator determines the reference current I_q and the reference torque. The regulator output is a control signal which indicates the reference current I_q .

The proposed control is explicated in "Fig. 2 "[23]

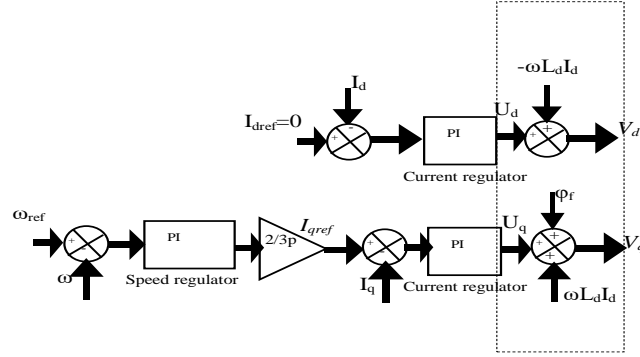


Fig. 2. Control principle diagram.

5. Backstepping Control

The equation (6) model is used to model PMSG. Because of the connection between current and velocity, the model has substantial nonlinearity. Backstepping control's core principle is to make the system flow in a first-order cascade stable subsystem in the sense of Lyapunov, giving it resilience and global asymptotic stability. The goal is to control the speed by using the dI_d/dt and dI_q/dt expressions as subsystems and the stator currents as intermediate variables (I_d , I_q). We can then compute the voltage commands (V_d , V_q) that are required to assure the PMSM's (Permanent Magnet Synchronous Machine) speed control as well as the overall system's stability. The following expressions illustrate the errors [1], [24]:

$$\begin{aligned}\xi_d &= I_d^* - I_d \\ \xi_q &= I_q^* - I_q \\ \xi_\Omega &= \Omega^* - \Omega\end{aligned}\tag{13}$$

And the dynamics of the errors are given as follows:

$$\begin{aligned}\dot{\xi}_d &= \dot{I}_d^* - \dot{I}_d \\ \dot{\xi}_q &= \dot{I}_q^* - \dot{I}_q \\ \dot{\xi}_\Omega &= \dot{\Omega}^* - \dot{\Omega}\end{aligned}\tag{14}$$

With;

$$\begin{aligned}\dot{I}_d^* &= 0 \\ \dot{I}_q^* &= 0\end{aligned}\tag{15}$$

step1: Backstepping speed controller

In the first step, by the Lyapunov functions (eq16) a virtual control is created to ensure that the system converges towards its equilibrium state:

$$V_1 = \frac{1}{2} \cdot \xi_{\Omega}^2 \quad (16)$$

The first derivation of Lyapunov function:

$$\begin{aligned} \dot{V}_1 &= \xi_{\Omega} \cdot \dot{\xi}_{\Omega} \\ &= -K_{\Omega} \cdot \xi_{\Omega}^2 + \frac{\xi_{\Omega}}{J} \left(-T_{tur} + F \cdot \Omega + K_{\Omega} \cdot J \cdot \xi_{\Omega} + \frac{3}{2} \cdot p \cdot I_q \cdot \varphi_f \right) \\ &\quad + \frac{3}{2J} \cdot p \cdot (L_d - L_q) \cdot I_d \cdot I_q \cdot \xi_{\Omega} \end{aligned} \quad (17)$$

With:

$$\xi_{\Omega} = \dot{\Omega}^* - \frac{1}{J} \left(T_{tur} - \frac{3}{2} \cdot p \cdot ((L_d - L_q) \cdot I_d \cdot I_q + I_q \cdot \varphi_f) - F \cdot \Omega \right) \quad (18)$$

Where

T_{tur} : turbine torque, K_{Ω} : rotational speed gain.

The first subsystem is stable; the derivative of the norm must always be negative $V_1 < 0$. This translates into the correct choice of stator currents values I_d and I_q .

$$\begin{aligned} I_d^* &= 0 \\ I_q^* &= \frac{2 \cdot J}{3 \cdot p \cdot \varphi_f} \left[-K_{\Omega} \cdot \xi_{\Omega} - \dot{\Omega}^* - \frac{T_{tur}}{J} - \frac{F}{J} \cdot \Omega \right] \end{aligned} \quad (19)$$

With:

$$\begin{aligned} \dot{\Omega}^* &= 0 \\ \dot{V}_1 &= -K_{\Omega} \cdot \xi_{\Omega}^2 \leq 0 \end{aligned} \quad (20)$$

Step2: Backstepping voltage controller

In this step, the control voltages statorique in Park axis V_d (Direct voltage) and V_q (Quadratic voltage) will be calculated based on the virtual entrances of the system. A new Lyapunov function based on the velocity tracking error and current component error to find the stator voltage references [9]:

$$V_2 = \frac{1}{2} \cdot (\xi_d^2 + \xi_q^2 + \xi_\Omega^2) \quad (21)$$

$$\dot{V}_2 = \xi_q \cdot \dot{\xi}_q + \xi_d \cdot \dot{\xi}_d + \xi_\Omega \cdot \dot{\xi}_\Omega = -K_\Omega \cdot \xi_\Omega^2 - K_d \cdot \xi_d^2 - K_q \cdot \xi_q^2$$

Using the previous equations, we get;

$$\dot{\xi}_d = \frac{1}{L_d} \cdot (R_d \cdot I_d - p \cdot \Omega \cdot L_q \cdot I_q - V_d) \quad (22)$$

$$\dot{\xi}_q = \frac{2}{3 \cdot p \cdot \varphi_f} \left((K_\Omega \cdot J - F) \left[T_{tur} - F \cdot \Omega - \frac{3 \cdot p}{2} \cdot \left((L_d - L_q) \cdot I_d \cdot I_q + I_q \cdot \varphi_f \right) + \frac{1}{L_q} \cdot (R_q \cdot I_q + p \cdot \Omega \cdot L_d \cdot I_d - V_q) \right] \right)$$

$$\dot{\xi}_\Omega = \frac{1}{J} \left[-K_\Omega \cdot J \cdot \xi_\Omega - \frac{3 \cdot p}{2} \varphi_f \cdot \xi_q - \frac{3 \cdot p}{2} \cdot (L_d - L_q) \cdot I_q \cdot \xi_d \right]$$

The choosing of the Current gains (d, q) Kd and Kq among the positive constants Contributes to system stability.[18]

In the end, the control laws are in the following forms:

$$I_q^* = -\frac{2 \cdot J}{3 \cdot p \cdot \varphi_f} \left[-K_\Omega \cdot \xi_\Omega - \dot{\Omega}^* - \frac{T_{tur}}{J} - \frac{F}{J} \cdot \Omega \right] \quad (23)$$

$$V_d = -L_d \left(-K_d \cdot \xi_d - \frac{R_d}{L_d} \cdot I_d + \frac{L_q}{L_d} \cdot I_q \cdot \omega \right)$$

$$V_q = -L_q \left(-K_q \cdot \xi_q - \frac{3 \cdot p \cdot \varphi_f}{2 \cdot J} \cdot c_\Omega - \frac{\varphi_f}{L_d} \cdot \omega - \frac{L_d}{L_q} \cdot I_d \cdot \omega - \frac{R_q}{L_q} \cdot I_q \right)$$

6. Fuzzy logic control

The use of this technique, first described by Lotfi Zadeh (1965), has become a viable alternative to several control systems in recent decades. Fuzzy logic techniques are now used in practically every sector and may be used to operate wind turbines with nonlinear models. The fuzzy logic structure is divided into three sub-blocks, as illustrated in Fig. 3, fuzzification, inference, and defuzzification [25].

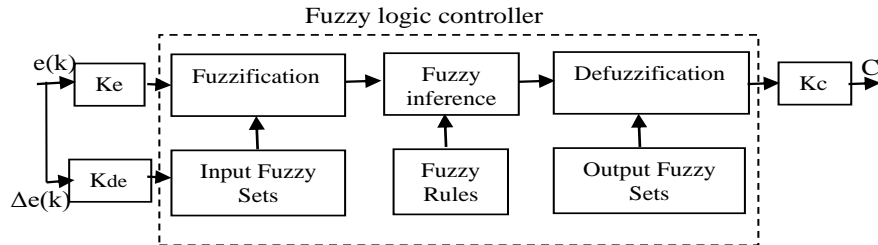


Fig. 3. Structure of the FLC

K_e , K_{de} , K_c They are scaling factors that can be constants or variables and play an important role in FLC design to achieve a good response in both dynamic and transient states.

Fuzzification

Based on a membership function, the numerical input variables ($e(k)$, $\Delta e(k)$) are converted into linguistic variables in this stage. There are seven levels of fuzziness employed; ZE (Zero), PB (Positive Big), PM (Positive Mean) PS (Positive Small), NB (Negative Big), NM(Negative Mean), and NS (Negative Small) [26], as illustrated in fig.4.

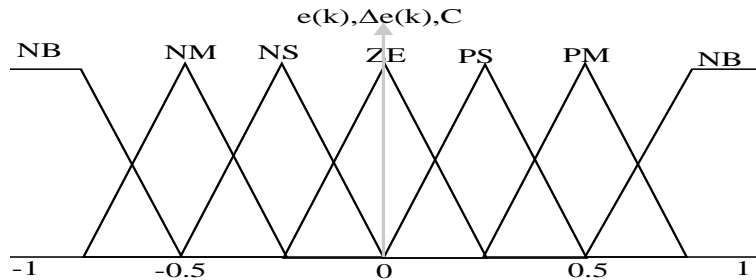


Fig.4. Membership functions for variables linguistics of the FLC

Fuzzy Rule Base

The table below gives 49 inference rules of different combinations between the variables linguistics $e(k)$, $\Delta e(k)$ with the output C to get the required reference signals [27]. The IF-THEN rules of the following types indicate the fuzzy mapping of the input variables to the output variable:
IF [$e(k)$ is NB] and [$\Delta e(k)$ is NB] THEN [C is PB].

IF [e(k) is PB] and [Δe(k) is PB] THEN [C is NB].[28]

Table 1

		Fuzzy rule table for FLC						
		NB	NM	NS	ZE	PS	PM	PB
e(k)	Δe(k)	PB	PB	PM	PM	PS	PM	ZE
NB		PB	PB	PM	PM	PS	PM	ZE
NM		PB	PM	PM	PS	PS	ZE	NS
NS		PM	PM	PS	PS	ZE	NS	NS
ZE		PM	PS	PS	ZE	NS	NS	NM
PS		PB	PS	ZE	NS	NS	NM	NM
PM		PS	ZE	NS	NS	NM	NM	NB
PB		PS	NS	NS	NM	NM	NB	NB

Inference and Defuzzification

This approach transforms the inferred fuzzy control action to a numerical variable at the output using the eq (24) by constructing the union of the outputs of each rule.[29, 30, 31, 32, 33].

$$\overline{M_n} = \frac{\sum_{i=1}^N \mu_i C_i}{\sum_{i=1}^N \mu_i} \quad (24)$$

Where;

N: number of rules.

μ_i : designates the membership rank.

C_i : the coordinate linked to the respective output.

7. Simulation results

The simulation model of wind conversion system with different control was created using the MATLAB/Simulink program.

Table 2

Parameters of the WECSs.	
Rd, Rq	0.5(Ω)
Ld, Lq	0.016(H)
Multiplier gain G	1
ρ	1.2255(kg.m ³)

Φ_f	0.148Wb
P	17
F	0.001 (N.s/rad)
J	0.021(kg.m ²)
S	$\Pi.R^2(m^2)$

We initially built vector control and backstepping control to make the system as resistant to structural uncertainty as feasible. The collected findings suggest that the backstepping control performs significantly better than the FOC, as shown in the figures below. By comparing the reference tracking in the two controls, the reference tracking in the backstepping control is more accurate than the tracking in the vector control. Furthermore, the initial oscillation of the Ω backstepping control is minimal.

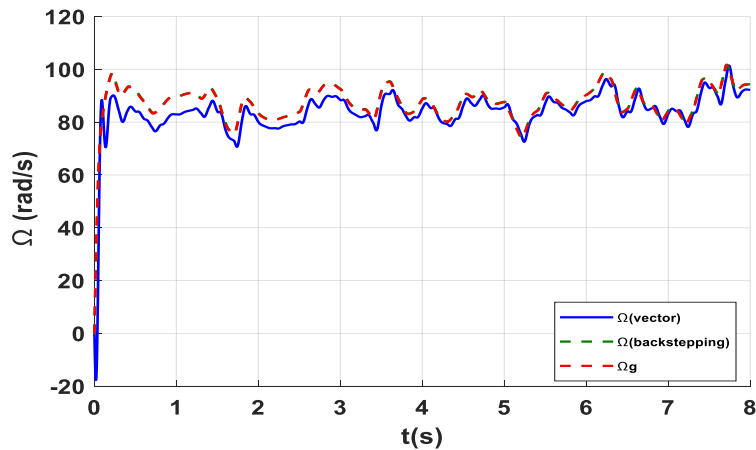
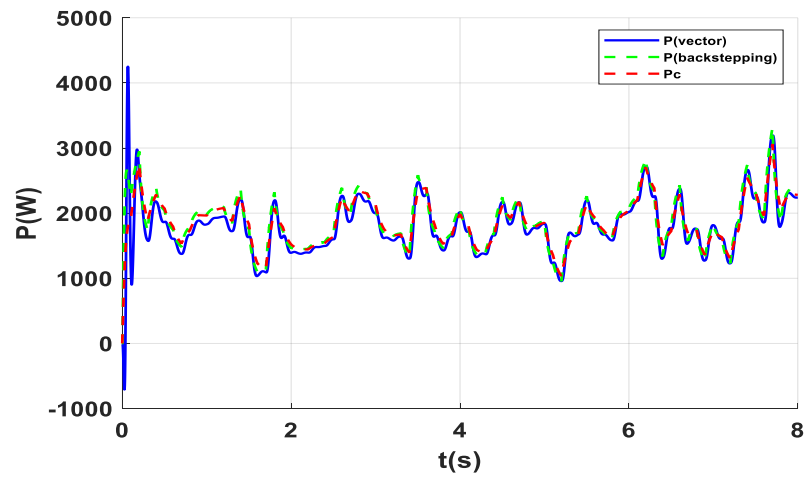
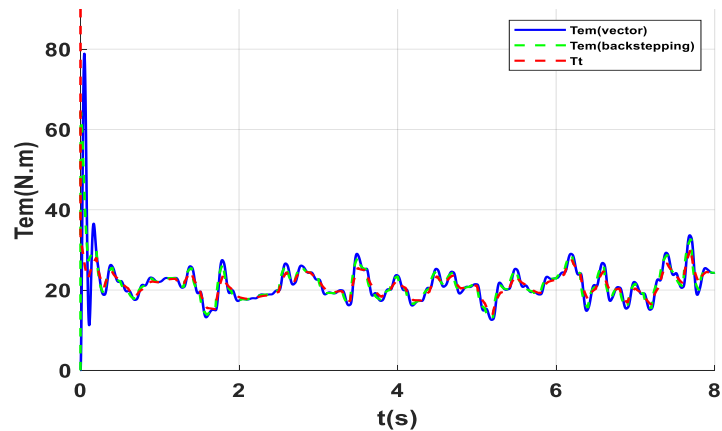
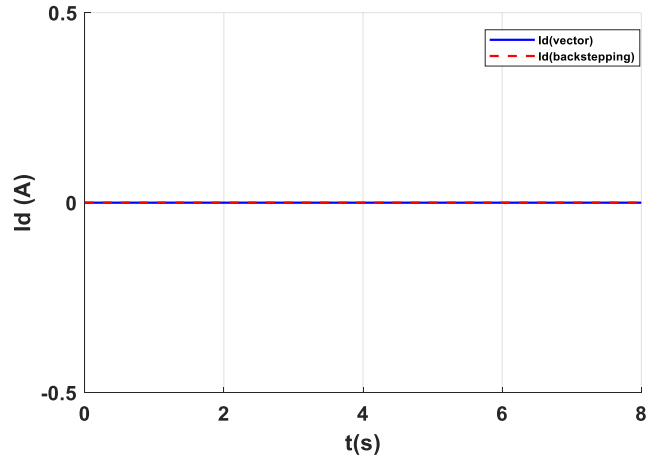
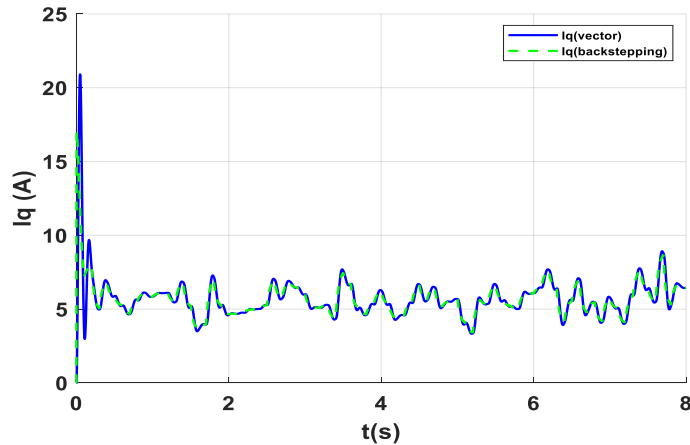


Fig.5. Rotation speed Ω (rad/s).

Fig.6. Powers generated P (Watt).Fig.7. Torque Tem and Tt (N.m).

Fig.8. Stator current I_d (A).Fig.9. Stator current I_q (A).

We will proceed to two increases of the parameters likely to change over time, namely the resistances R_d and R_q (assumption of generator heating with time) and the inductances L_d and L_q (assumption of saturation) as shown in (fig.10.a, b) for study the variations of the different quantities according to the applied stresses and to analyze the extreme conditions of operation.

At $t=3$ sec: Increase in resistances by 10% and inductances by 7%.

At $t=5$ sec: Increase in resistances by 50% and inductances by 14%.

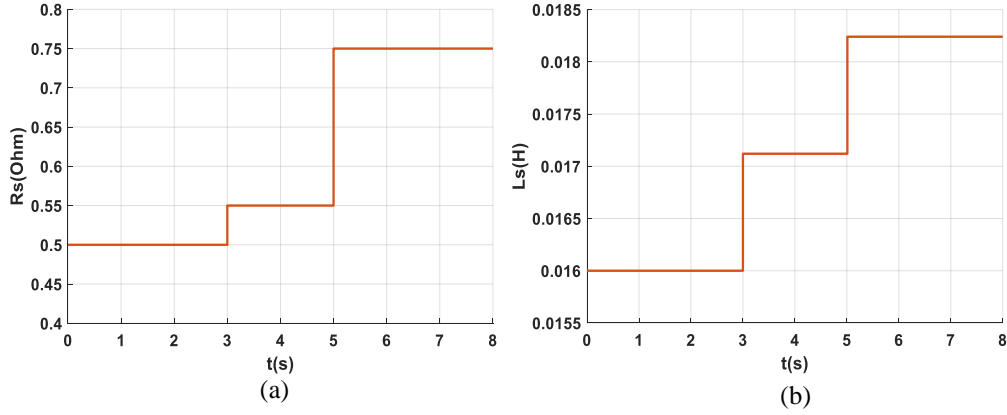
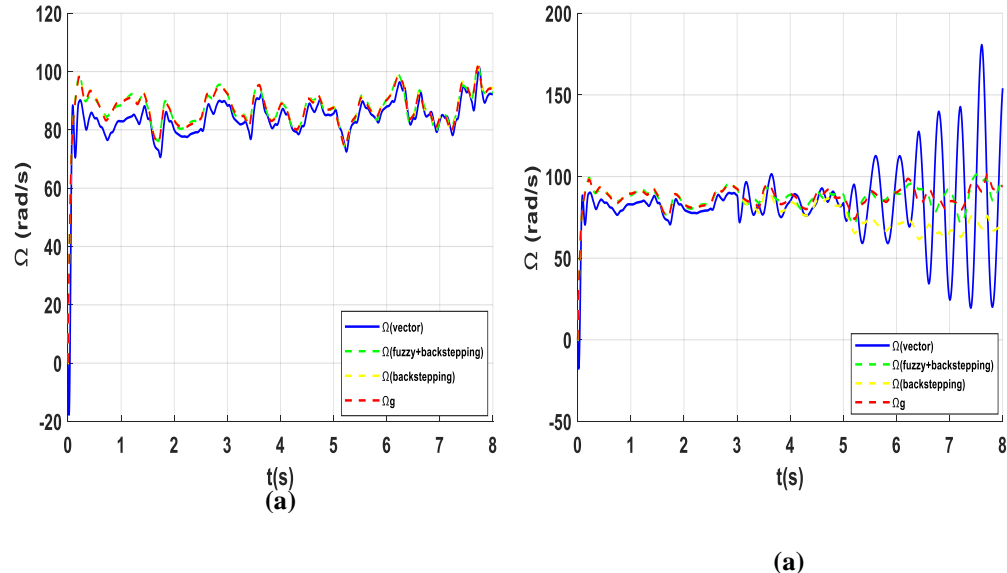
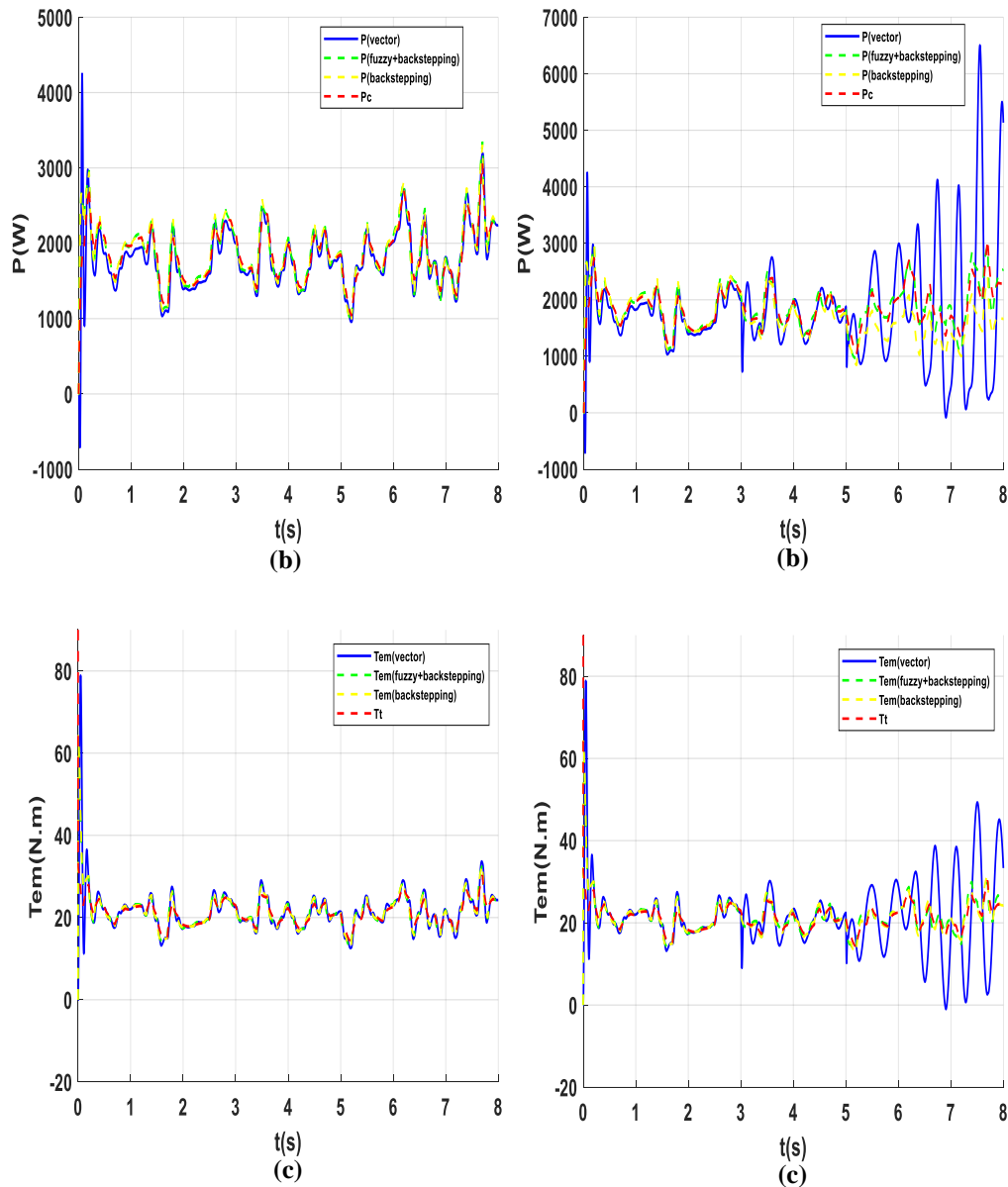


Fig.10. (a): Variation of stator resistances (R_d , R_q) (Ohm), (b):Variation of stator inductances (L_d , L_q) (H).

The figures below show us the results of the simulation of various Controls made in this article (FOC, Backstepping, fuzzy-backstepping) was carried out without and with variation of the machine parameters.





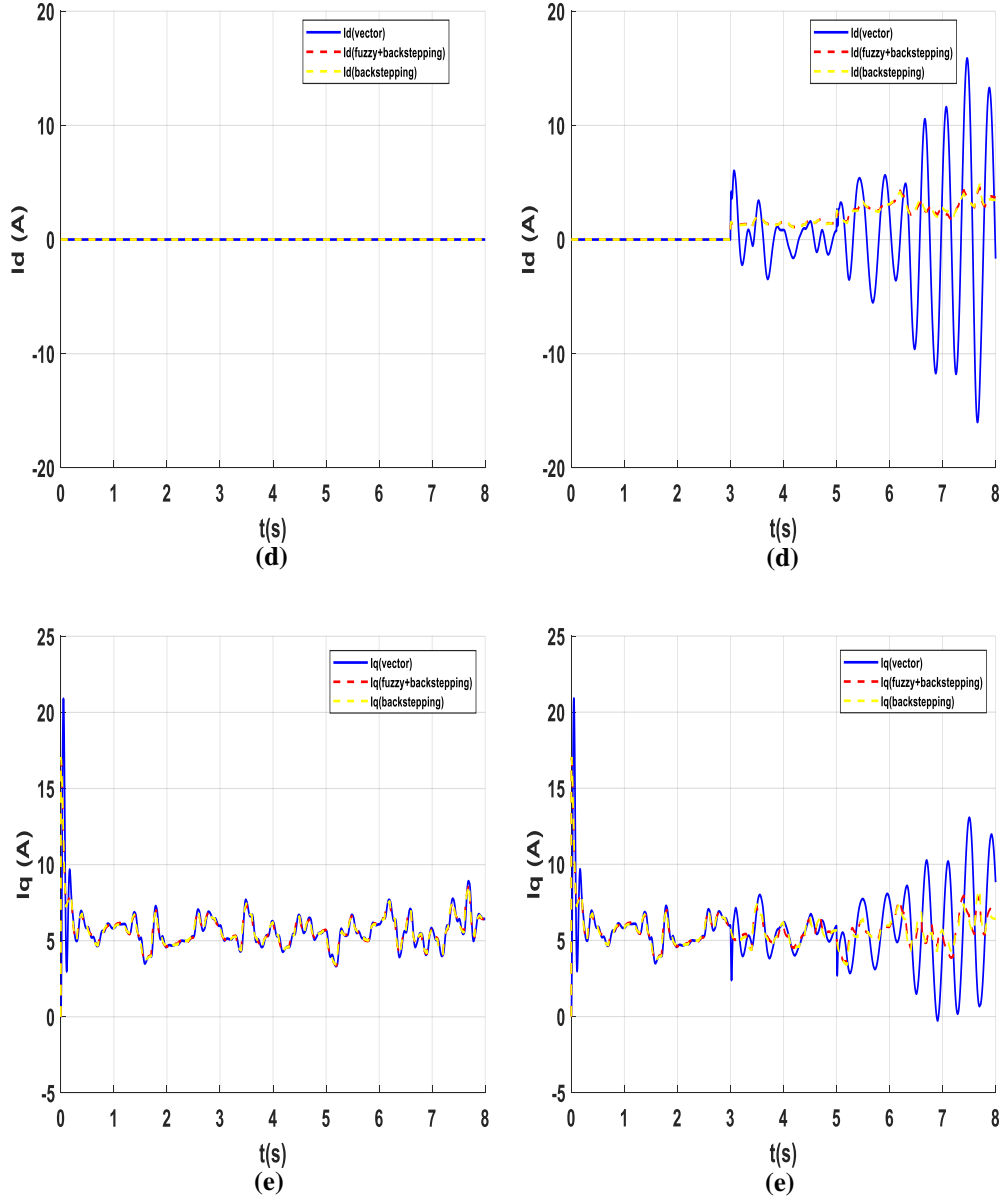


Fig.11. The different control without variations of stator parameter (R,L) (a) rotation speed, (b) power generated, (c) electromagnetic torque, (d) stator current I_d and (e) stator current I_q

Fig.12. The different control under variations of stator parameter (R,L) (a) rotation speed, (b) power generated, (c) electromagnetic torque, (d) stator current I_d and (e) stator current I_q

(Fig.11) and (Fig.12) show a comparison between the simulation results of different control applied on the wind turbine based on a PMSG with and without variation of the stator parameter.

The (Fig.11.a), (Fig.11.b) and (Fig.11.c), show the shape of the speed, power, and torque, where it is noted that the vector control in the three figures follows the reference value with a limited offset at the beginning for the speed and power, but they follow the set point perfectly in backstepping and fuzzy-backstepping control (more efficient in the backstepping control). As for the current I_d , it remains zero in operation without applying the constraints (Fig.11.d), before the oscillations, increase when the constraints are applied (Fig.12.d). When we apply the constraints (Fig.12) at $t=3\text{sec}$ (R increases (10%) and L increases (7%)) we see a limited distortion compared to the vector control. An increase in the value of R and L ($R(50\%)$ and $L(14\%)$) produces in the form of vector control (Fig.12.a) and (Fig.12.b), quite significant oscillations appear around the reference value. For the electromagnetic torque (Fig.12.c), we notice a deterioration of the tracking; similarly, for the current I_q (Fig.12.e), which is the image of the torque. In (Fig.12.a),(Fig.12.b) the result is good in fuzzy-backstepping where the tracking of the reference is more accurate compared to the backstepping control, and opposite to the FOC with which the tracking is bad from that moment on. The torque (Fig.12.c) and the current I_q (Fig.12.e) behave well. The current I_d (Fig.12.d) is perturbed but slightly less than the vector control. Thus, the results show that, compared to the vector control and the Backstepping-Fuzzy combination, the results obtained by the Backstepping control are the most efficient without constraints. When we apply constraints, first at the 3rd second and then at the 5th second, we find that the Backstepping-Fuzzy control combination is the best compared to the vector control and the Backstepping control.

8. Conclusion

This paper proposes robust control techniques for WECSs to improve the performance of a PMSG. We first used vector control, which showed quite limited results in terms of monitoring. In order to overcome the shortcomings of vector control, we have thought of new intelligent control technology, in particular backstepping control and fuzzy logic control (associated backstepping -fuzzy). These smart controls have shown excellent results, especially in terms of flexibility and adjustment. The results show that, compared to vector control and Backstepping-Fuzzy associations, the number of backstepping control is the most efficient without constraints. When applying the Backstepping-fuzzy combination constraints to the GSAP machine, the simulation gave us a good result, showing perfect tracking response and robustness to changes in stator parameters.

Acknowledgement

The authors would like to thank the Directorate General for Scientific Research and Technological Development (DGRSDT) for the support and funding of the research axis through the LDDI research laboratory.

R E F E R E N C E S

- [1]. *Y.El Mourabit, et al* “Implementation and validation of backstepping control for PMSG wind turbine using dSPACE controller board”, Energy Reports 5 (2019) 807–821
- [2]. *Mohamed Baha Eddine Zarrouki, Said Benaggoune, Rachid Abdesselam*, “Stratégie de contrôle non linéaire optimisée pour le générateur synchrone à aimant permanent (gsap) dans le système de conversion de l'énergie éolienne (SCEE), U.P.B. Sci. Bull., Series C, Vol. 83, Iss. 1, 2021 ISSN 2286-3540.
- [3]. *Z. Zhongming, et al.* “Global wind power growth must triple over next decade to achieve Net Zero” 2021.
- [4]. *G.Debastiani, et al* “Assessment of the energy efficiency of a hybrid wind-photovoltaic system for Cascavel, PR” Renewable and Sustainable Energy Reviews 131 110013, 2020.
- [5]. *F. Tahiri, A. Harrouz et al* "Technique of Control Pmsm Powered by Pv Panel Using Predictive Controller of Dtc-Svm." *Facta Universitatis, Series: Electronics and Energetics* 33.3: 429-444, 2020.
- [6]. *H. Nguyen, A S. Al-Sumaiti et al* “Optimal power tracking of PMSG based wind energy conversion systems by constrained direct control with fast convergence rates” Electrical Power and Energy Systems 118 ,105807, 2020.
- [7]. *H.Gallas, et al* “Robust Control and harmonics modeling of a PMSG for a 1.5 MW wind turbine” International Conference on Electrical Machines (ICEM) (Vol. 1). IEEE, 2020.
- [8]. *H. Becheri, I. K. Bousarhanne, A. Harrouz, I Colak, K Kayisli*, “Sensorless Control of Wind Turbine Conversion Equipped with a DFIG Using MPPT Strategy”, Journal "IEEE Explore" of 18th International Power Electronics and Motion Control Conference (PEMC), Budapest, Hungary 26-30 Aug. 2018, Pages: 605 – 610.
- [9]. *A. Harrouz, K Nourdine, K Kayisli, HI Bulbul, I Colak*, “A Fuzzy Controller for Stabilization of Asynchronous Machine”, Journal "IEEE Explore" of 7th International Conference on Renewable Energy Research and Application (ICRERA2018), Paris, 2018.
- [10]. *Y. El Mourabit, O. Zamzoum et al* “Dynamic modeling and control of a wind turbine with MPPT control connected to the grid by using PMSG” 3rd International Conference on Advanced Technologies for Signal and Image Processing , Fez, Morocco.- ATSIP'2017.
- [11]. *Y. Zahraoui, et al.* “Induction motor harmonic reduction using space vector modulation algorithm.” Bulletin of Electrical Engineering and Informatics 9.2 (2020): 452-465.
- [12]. *Becheri Hocine, Boughazi Othmane, A. Harrouz*, “Commande de la Machine Asynchrone par la Technique Directe du Couple-Backstepping avec Onduleur à Modulation Vectorielle Spatiale’, Revue roumaine des sciences techniques, V. 64 NO 1 , pp.81-86, 2019.
- [13]. *C-I.Nicola, et al* “Sensorless Control of PMSM Based on Backstepping-PSO-Type Controller and ESO-Type Observer Using Real-Time Hardware” Electronics 2021, 10, 2080
- [14]. *T Z.Farge, et al* “Vector Control of Low Power HAWT Based PMSG Using SVPWM Under Variable Wind Speeds” 2nd International Conference on Electromechanical Engineering and its Applications (ICEMEA-2021), University of Technology /Iraq-Baghdad.2021
- [15]. *R. Abbas, A. Harrouz, D. Belatrache, V. Dumbrava*, ‘Simulation and Optimization of a Wind Energy System in the Adrar Region’. Algerian Journal of Renewable Energy and Sustainable Development, 3(02), 198-215, 2021.

- [16]. *M S. Eslahi, S. Vaez-Zadeh, A. Jabbarnejad* “A Comparative Study of Control Methods for Grid Side Converters in PMSG-Based Wind Energy Conversion Systems” IEEE 29th International Symposium on Industrial Electronics (ISIE) 2020.
- [17]. *S E. Rhaili, A. Abbou et al* “Robust Sliding Mode Control with Five Sliding Surfaces of Five-Phase PMSG Based Variable Speed Wind Energy Conversion System” International Journal of Intelligent Engineering and Systems, Vol.13, No.4, 2020.
- [18]. *A. Harrouz, H Becheri, I Colak, K Kayisli*, “Backstepping control of a separately excited DC motor”, Electrical Engineering, Springer Berlin Heidelberg, ISSN: 0948-7921, Vol.100, Issue 3, September 2018, pp. 1393-1403.
- [19]. *Y.El Mourabit, A.Derouich* “Nonlinear backstepping control for PMSG wind turbine used on the real wind profile of the Dakhla-Morocco city” Int Trans Electr Energ Syst. e12297.2020.
- [20]. *M. Fannakh, M L. Elhafyani et al* “Overall fuzzy logic control strategy of direct driven PMSG wind turbine connected to grid” International Journal of Electrical and Computer Engineering (IJECE) Vol. 11, No. 6, pp. 5515~5529. December 2021.
- [21]. *F. Tahiri, F. Bekraoui, Boussaïdi., Ouledali O., A. Harrouz*, “Direct Torque Control (DTC) SVM Predictive of a PMSM Powered by a Photovoltaic Source”, Algerian Journal of Renewable Energy and Sustainable Development, 1(01), 1-7, 2019.
- [22]. *A. Harrouz, Ilhami Colak, Korhan Kayisli*, “Control of a small wind turbine system application”, Journal “IEEE Xplore” of IEEE International Conference on Renewable Energy Research and Applications (ICRERA), 2016, Pages: 1128 – 1133.
- [23]. *W. Torki, et al* “Vector control of a PMSG direct-drive wind turbine”. In 2017 International Conference on Green Energy Conversion Systems (GECS) (pp. 1-6). IEEE. (2017, March).
- [24]. *E. Mahersi, A. Khedher* “Backstepping flux observer for nonlinear control of the direct-drive permanent magnet synchronous generator wind turbines”. Wind Engineering, 40(6), 540-554.2016
- [25]. *B. Kanouni, S.Mekhilef* “Fuzzy logic MPPT control algorithm for a Proton Exchange Membrane Fuel Cells System”. Algerian Journal of Renewable Energy and Sustainable Development, 3(01), pp. 13-22, 2021.
- [26]. *Cheggaga N., Benallal A., & Tchoketch KebirS..* A New Neural Networks Approach Used to Improve Wind Speed Time Series Forecasting. Algerian Journal of Renewable Energy and Sustainable Development, 3(02), pp.151-156, 2021.
- [27]. *M. Soliman, et al* “An adaptive fuzzy logic control strategy for performance enhancement of a grid-connected PMSG-based wind turbine”. IEEE Transactions on Industrial Informatics, 15(6), 3163-3173.2018.
- [28]. *F. Bourourou, S.A. Tadjer, I. Habi* “Wind Power Conversion Chain Harmonic Compensation using APF Based on FLC”. Algerian Journal of Renewable Energy and Sustainable Development, 2(01), 75-83.2020.
- [29]. *L. Zaghiba, M. Khennane, A. Borni, A. Fezzani* “Intelligent PSO-Fuzzy MPPT approach for Stand Alone PV System under Real Outdoor Weather Conditions”. *Alger. J. Renew. Energy Sustain. Dev*, 3, 1-12. (2021).
- [30] *A. Harrouz, F. Tahiri, F. Bekraoui, and I. Boussaid*, “Modelling and Simulation of Synchronous Inductor Machines.”, Algerian Journal of Renewable Energy and Sustainable Development, 1(01), 8-23. (2019).
- [31] *I. Boussaid, A. Harrouz, and P. Wira*, "Advanced Control of Doubly Fed Induction Generator for Wind Power Systems: Optimal Control of Power Using PSO Algorithm," Applied Mechanics and Materials, vol. 905, pp. 29-42, 2022, **DOI:** <https://doi.org/10.4028/v-era743>
- [32] *M. Bouzidi, A. Harrouz, S. Mansouri and V. Dumbrava*, “Modeling of a Photovoltaic Array with Maximum Power Point Tracking Using Neural Networks”, Applied Mechanics and Materials, vol. 905, pp. 01-06, 2022, **DOI:** <https://doi.org/10.4028/v-era743>

[33] *T. Nawal, B. Bachir, C. Saliha, , A. Harrouz and R. El-Sehiemy*, “Renewable Energy Sources Scheduling Approach for Windfarm Layout Optimization by Using Ant Lion Optimization Algorithm” *Applied Mechanics and Materials*, vol. 905, pp. 01-06, 2022, **DOI:** <https://doi.org/10.4028/v-era743>